Original Article

Application of Texture Analysis Method for Classification of Benign and Malignant Thyroid Nodules in Ultrasound Images

Ali Abbasian Ardakani[1], Akbar Gharbali[2], Afshin Mohammadi[3]

Abstract

Background: The aim of this study was to evaluate computer aided diagnosis (CAD) system with texture analysis (TA) to improve radiologists' accuracy in identification of thyroid nodules as malignant or benign.

Methods: A total of 70 cases (26 benign and 44 malignant) were analyzed in this study. We extracted up to 270 statistical texture features as a descriptor for each selected region of interests (ROIs) in three normalization schemes (default, 3σ and 1%-99%). Then features by the lowest probability of classification error and average correlation coefficients (POE+ACC), and Fisher coefficient (Fisher) eliminated to 10 best and most effective features. These features were analyzed under standard and nonstandard states. For TA of the thyroid nodules, Principle Component Analysis (PCA), Linear Discriminant Analysis (LDA) and Non-Linear Discriminant Analysis (NDA) were applied. First Nearest-Neighbour (1-NN) classifier was performed for the features resulting from PCA and LDA. NDA features were classified by artificial neural network (A-NN). Receiver operating characteristic (ROC) curve analysis was used for examining the performance of TA methods.

Results: The best results were driven in 1-99% normalization with features extracted by POE+ACC algorithm and analyzed by NDA with the area under the ROC curve (A_z) of 0.9722 which correspond to sensitivity of 94.45%, specificity of 100%, and accuracy of 97.14%.

Conclusion: Our results indicate that TA is a reliable method, can provide useful information help radiologist in detection and classification of benign and malignant thyroid nodules.

Keywords: ultrasonography; thyroid nodule; Diagnosis, Computer-Assisted; Artificial Intelligence

Please cite this article as: Abbasian-Ardakani A, Gharbali A, Mohammadi A. Application of Texture Analysis Method for Classification of Benign and Malignant Thyroid Nodules in Ultrasound Images. Iran J Cancer Prev. 2015;8(2):116-24.

1. Student Research Committee, Urmia University of Medical Sciences, Urmia, Iran
2. Dept. of Medical Physics, Faculty of Medicine, Urmia University of Medical Sciences, Urmia, Iran
3. Dept. of Radiology, Faculty of Medicine, Imam Khomeini Hospital, Urmia University of Medical Sciences, Urmia, Iran

Corresponding Author:
Akbar Gharbali, PhD;
Assistant Professor of Medical Physics
Tel: (+98) 4412780801, (+98) 9149358500
Email: Gharbali@yahoo.com
Received: 06 Oct. 2014
Accepted: 24 Dec. 2014
Iran J Cancer Prev. 2015; 2:116-24.

Introduction

Thyroid nodules have an incidence of 33-68% in the general population and can be malignant or benign; however, 5-15% of these nodules are malignant [1, 2]. Although the incident of palpable thyroid nodules in the adult population ranges from 4 to 8%, at autopsy 50% of the population has thyroid nodules [3]. Many techniques like physical examination, fine needle aspiration cytological examination and imaging are used to detect thyroid nodules. A fine needle aspiration biopsy (FNAB) is a non-surgical and accepted diagnostic method for confirming the nature of the nodules. However, it leads to 10% to 20% thyroid nodules with no diagnosis and 15-30% of results are indeterminate. Non-diagnostic FNAB indicates that thyroid nodules have a high probability of malignancy and aspiration should be repeated [2, 4].

Radiographs, computed tomography (CT), magnetic resonance imaging (MRI), positron emission tomography (PET), ultrasound and scintigraphy are diagnostic imaging modalities available for the evaluation of thyroid nodules. Ultrasound is the chosen imaging technique for assessment of thyroid nodules, owing to being in real time, radiation-free, non-invasive, widely available, low cost and ability to detect non-palpable

nodules [5]. Nowadays, high frequency transducers provide high definition images and spatial resolution. Grey-scale ultrasound contains useful features to quantitatively characterize thyroid nodules such as texture features, whereas Doppler provides an intra-nodal vascular pattern [6, 7].

Although there is no precise and mathematical definition of texture, simply conceived by human. Image texture can be described by various patterns: coarse, fine, smooth, spatial variations in pixel intensity of objects within an image. Contrary to the computer, human detection of textures may be qualitative and limited by vision. Likewise such patterns within the image may be different but will be perceived by humans as the same texture. Computerized texture analysis (TA) is a mathematical technique that increases and provides rich quantification and information of spatial grey-level intensities in pixels within the image [8-10]. Initial diagnosis by a radiologist is qualitative and may contain errors. To increase and improve the confidence of a radiologist in differentiating between benign and malignant thyroid nodules, computer aided diagnosis (CAD) systems have been developed.

Hong et al. [11] used real-time ultrasound elastography to classify benign from malignant thyroid nodules with a sensitivity of 88%, specificity of 90%, PPV of 81%, NPV of 93% and an area under the ROC curve (A_z) of 0.94. Ding et al. reported that sensitivity, specificity and accuracy were 94.6%, 92.8% and 93.6% respectively when the energy features of co-occurrence matrix were used. Tsantis *et al*. [12] Tsantis et al. used speckle-free feature set based on nodules' boundary shape and 'wavelet local maxima located' for differentiating between benign and malignant thyroid nodules with a sensitivity of 93%, specificity of 98%and an area under the ROC curve (A_z) of 0.96. Gopinath et al. [13] utilized texture features derived from the Gabor filter bank at various wavelengths and angles for the classification of benign and malignant thyroid nodules. They used SVM classifier and achieved the sensitivity of 95%, specificity of 100% and accuracy of 96.7%. Gopinath et al. [14] reported that accuracy, sensitivity, and specificity were 90%, 100%, and 90% respectively when two-level wavelet decomposition based on the texture characteristics of the thyroid cells was used to differentiate between benign and malignant thyroid nodules.

In this study, we evaluated a non-invasive method based on TA to improve radiologists' diagnosis in the classification of thyroid nodules as benign or malignant in ultrasound images. Although our study is not the first attempt to use a TA method, as far as we know no other study has employed TA via all groups and classes of texture features.

Materials and Methods

Ultrasound images of 70 patients (53 female, and 17 male) comprising 26 benign (colloid and adenomatous nodules) and 44 malignant thyroid nodules (41 papillary thyroid carcinoma and 3 hurtle cell carcinoma) which had been approved by FNAB. Ultrasound guided needle aspiration were used based on clinical indication. Thyroid nodules images saved in ultrasonography system and the images were compared with biopsy and the reference for statistical analysis. The databases were selected in the time interval from June 2013 to August 2014 in the Radiology department of Imam Khomeini hospital, Urmia, Iran.

Ultrasound images were acquired by Accuvix V20 sonography system (Medison, Seoul, Korea) equipped by L5-13IS linear array transducer working in the range 5-13MHz. Ultrasound images were input to MaZda software (MaZda 4.6, The Technical University of Lodz, Institute of Electronics) for TA [15]. We have selected one region of interest (ROI) for each ultrasound image; hence 70 non-overlapping ROIs (26 benign and 44 malignant) were selected in Mazda for TA. We evaluated and analyzed texture features coming from six main categories for differentiating between benign and malignant thyroid nodules: Histogram (statistical class), Absolute gradient (statistical class), Run-length matrix (statistical class), Co-occurrence matrix (statistical class), Auto-Regressive model (model class) and Wavelets (transform class) [9].

Up to 270 texture features are extracted for each ROI in three normalization schemes. N_1: default. Default images had the same appearance. An intensity range will be from 1 to 2^k, where k is the number of the bits per pixel. N_2: 3σ, limiting image intensities in the range $[\mu-3\sigma, \mu+3\sigma]$ where μ is the mean grey level value and σ the standard deviation of the grey levels' intensity inside the ROI. N_3: the ROIs grey level ranges between the darkness level at which the image's accumulated histogram is

equal to 1% of its total to the brightness level, where accumulated histogram is equal to 99% of its total.

Automated Feature Selection

All 270 parameters are not suitable and effective for differentiating between benign and malignant thyroid nodules. By using two reduction algorithms, Fisher and lowest probability of classification error and average correlation coefficients (POE+ACC), these parameters were reduced to the best ten texture features to show the best discrimination between benign and malignant thyroid nodules [16, 17]. Fisher algorithm selected up to ten features, with the highest being a ratio of between-class variance (D) to within-class variance (V).

$$F = \frac{D}{V} = \frac{\frac{1}{1-\sum_{k=1}^{K} P_k^2} \sum_{k=1}^{K} \sum_{j=1}^{K} P_k P_j (\mu_k - \mu_j)^2}{\sum_{k=1}^{K} P_k V_k}$$

Where μ_k and V_k are mean and variance of class k, F is Fisher coefficient and P_k is probability of class k. Maximization of Fisher coefficient is desirable.

A POE+ACC algorithm produced set up ten features with minimization probability of classification error (POE) and average correlation coefficients (ACC) between chosen features. The first feature, f^1, is selected to minimize POE for all classes:

$$f^1 = f_i{:}min_i\,[POE(f_i)]$$

Where POE(f_i) is the classification error probability for feature f_i. This probability is defined as follows:

$$POE(f_i) = \frac{number\ of\ samples\ not\ properly\ classified, marked\ in\ figure\ 1}{total\ number\ of\ samples\ in\ analyzed\ data\ set}$$

Figure 1 shows the sample distribution of feature f_i for two classes. The samples marked can be assigned to both class 1 or 2. In this case, these samples cannot be properly classified. The next feature (second feature) is then selected by minimizing the sum of all features except, excluding f^1:

$$f^2 = f_i{:}min_i\,[POE(f_i) + |CC(f^1, f_i)|]$$

The $|CC(f^1,f_i)|$ is the absolute value of the correlation coefficient between the previously calculated feature f^1 and the new feature f_i. The n-th feature is selected by minimizing the following sum for all remaining features except for the already chosen features:

$$f^n = f_i{:}min_i\,[POE(f_i) + \frac{1}{n-1}\sum_{k=1}^{n-1}|CC(f^k, f_i)|] = min_i\,[POE(f_i) + ACC(f_i)]$$

Where the averaged sum is extended for all correlation coefficients between previously selected features and feature f_i. This sum is defined as an average correlation coefficient (ACC). In brief, the POE+ACC algorithm introduces ten features with high discriminatory potential and a least correlation with features that are already selected.

Texture Analysis Methods

LDA, PCA and NDA investigate these features and transform data to lower-dimensional spaces, and increase the discriminative power under two standardization states (standard and nonstandard) [18, 19]. PCA and LDA features were classified by 1-NN classifier and A-NN classifier was performed for the features resulting from NDA [20]. ROC curve analysis was employed to compare the discrimination performance of the applied TA methods using the area under the ROC curve (A_z) [21]. In addition, six objectives that indices sensitivity (SEN), specificity (SPC), overall accuracy (ACC), positive predictive value (PPV) and negative predictive value (NPV)were also applied to assess the performance of the proposed methods. These indices are defined as follows:

$$Accuracy(ACC) = N_{TN} + N_{TP}/N_{TN} + N_{FN} + N_{TP} + N_{FP}$$
$$sensitivity(SEN) = N_{TP}/N_{TP} + N_{FN}$$
$$Specificity(SPC) = N_{TN}/N_{TN} + N_{FP}$$
$$Positive\ Predictive\ Value(PPV) = N_{TP}/N_{TP} + N_{FP}$$
$$Negative\ Predictive\ Value(NPV) = N_{TN}/N_{TN} + N_{FN}$$

Where N_{TP} is the number of malignant cases and $N_{TN}$is the number of benign cases that have been diagnosed correctly. N_{FP} and N_{FN} are the number of incorrectly diagnosed benign and malignant cases, respectively. Figure 2 shows the steps of CAD processing.

Results

In this study a total of 70 patients including 26 benign and 44 malignant thyroid nodules were approved by FNAB to ensure the classification accuracy of the proposed method. As mentioned previously, in each normalization scheme the same TA method and the same classifier were applied to the set of features resulting from both POE+ACC and Fisher algorithm.

In default normalization, we found out the features extracted by POE+ACC algorithm and analyzed by NDA to be higher than the other two

Table 1. Summary of performance for different features and Method of feature reduction in default normalization.

Feature selection method	Method of feature reduction	SEN (%)	SPC (%)	ACC (%)	PPV (%)	NPV (%)	A_z value
Fisher	N. S. PCA	72.22	38.46	51.42	61.9	35.71	0.5534
	S. PCA	79.54	73.07	77.14	83.33	67.85	0.763
	N. S. LDA	81.82	65.38	75.71	80	68	0.736
	S. LDA	79.54	69.23	75.71	81.39	66.67	.7438
	NDA	94.28	96.42	95.6	94.28	96.42	0.9535
POE+ACC	N. S. PCA	85.71	85.71	85.71	78.94	90.56	0.8571
	S. PCA	85.71	87.5	86.81	81.08	90.74	0.866
	N. S. LDA	91.42	91.07	91.2	86.48	94.44	0.9124
	S. LDA	91.42	91.07	91.2	86.48	94.44	0.9124
	NDA	94.28	98.21	96.7	97.05	96.49	0.9625

SEN = sensitivity; SPC = specificity; ACC = accuracy; PPV = positive predictive value; NPV = negative predictive value; A_z= area under ROC curve.

Table 2. Summary of performance for different features and Method of feature reduction in 3sigma normalization.

Feature selection method	Method of feature reduction	SEN (%)	SPC (%)	ACC (%)	PPV (%)	NPV (%)	A_z value
Fisher	N. S. PCA	75	61.54	70	76.74	59.26	0.6827
	S. PCA	77.27	69.23	74.28	81	64.28	0.7325
	N. S. LDA	84.09	65.38	77.14	80.43	70.63	0.7473
	S. LDA	84.09	65.38	77.14	80.43	70.63	0.7473
	NDA	86.36	100	91.42	100	81.25	0.9318
POE+ACC	N. S. PCA	70.45	53.85	64.28	72.10	51.85	0.6215
	S. PCA	81.82	58	72.86	77.55	65.22	0.6991
	N. S. LDA	77.28	57.7	70	75.55	60	0.6749
	S. LDA	77.28	57.7	70	75.55	60	0.6749
	NDA	93.18	92.3	92.85	95.34	88.89	0.9274

SEN = sensitivity; SPC = specificity; ACC = accuracy; PPV = positive predictive value; NPV = negative predictive value; A_z= area under ROC curve.

TA methods, PCA and LDA. In this case we reached a sensitivity of 94.28%, specificity of 96.42%, accuracy of 95.6%, PPV of 94.28% and NPV of 96.42% (Table 1). In terms of the normalization role, in 3 sigma normalization the NDA has shown the best discrimination power with features resulting just from the Fisher algorithm, where sensitivity, specificity, accuracy, PPV and NPV were 86.36%, 100%, 91.42%, 100% and 81.25%, respectively (Table 2). In 1-99% normalization and features resulting from POE+ACC algorithm analyzed by NDA have the highest discrimination power to distinguish between benign and malignant thyroid nodules, with which sensitivity, specificity, accuracy, PPV and NPV were 94.45%, 100%, 97.14%, 100% and 92.86% respectively (Table 3).

Figure 3, 4 and 5 respectively represent ROC curves plotted on the same graph for each normalization and features resulting from reduction method to compare the discriminating power for

Table 3. Summary of performance for different features and Method of feature reduction in 1-99% normalization.

Feature selection method	Method of feature reduction	SEN (%)	SPC (%)	ACC (%)	PPV (%)	NPV (%)	value A_z
Fisher	N. S. PCA	72.73	53.85	65.71	72.73	53.85	0.6329
	S. PCA	72.73	53.85	65.71	72.73	53.85	0.6329
	N. S. LDA	84.09	80.77	82.85	88.01	75	0.8243
	S. LDA	84.09	80.77	82.85	88.01	75	0.8243
	NDA	86.36	100	91.43	100	81.25	0.9118
POE+ACC	N. S. PCA	72.73	53.85	68.57	72.73	53.85	0.6279
	S. PCA	86.36	50	72.86	74.5	68.42	0.6818
	N. S. LDA	81.82	69.23	77.14	81.82	69.23	0.7552
	S. LDA	81.82	69.23	77.14	81.82	69.23	0.7552
	NDA	94.45	100	97.14	100	92.86	0.9722

SEN = sensitivity; SPC = specificity; ACC = accuracy; PPV = positive predictive value; NPV = negative predictive value; A_z= area under ROC curve.

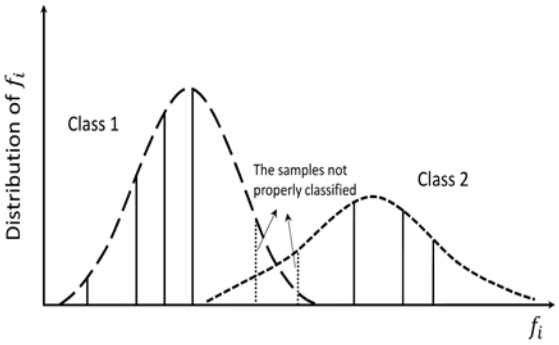

Figure 1. A sample distribution of feature f_i for two classes. The samples marked cannot be properly classified.

classification of benign and malignant thyroid nodules. In general, the NDA TA method has an advantage over PCA and LDA in each state with respect to a greater A_z value.

Discussion

In this study, three normalizations, two reduction algorithms, two standardization states and three TA methods provide a total of 36 states for each ROI case study. In our study, LDA has good performance with the features resulting from POE+ACC in default normalization in which A_z value is 0.9124 (Figure 3). However, PCA has

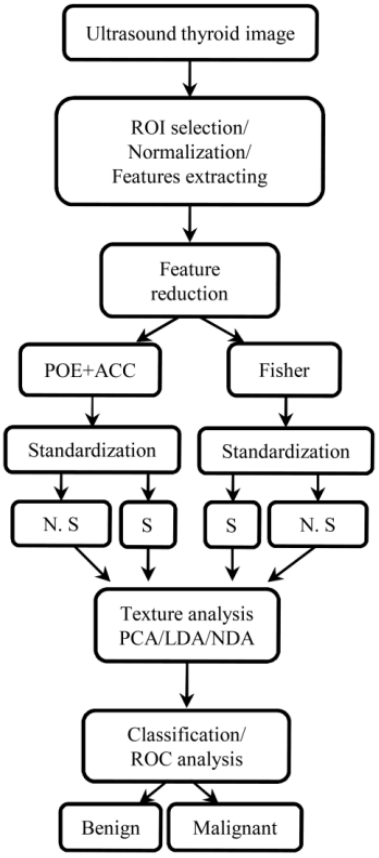

Figure 2. Overview of general texture analysis process in the ultrasound thyroid image.

undesirable results in comparison with LDA and NDA.

From Figures 3, 4 and 5 one can see that normalization has reflected a positive impact on the performance of the classifier. Hence the best performance in this study was obtained in 1-99% with NDA. The best results were driven in 1-99% normalization with features extracted by POE+ACC algorithm and analyzed by NDA with A_z value of 0.9722, which corresponds to a sensitivity of 94.45%, specificity of 100%, and accuracy of 97.14%. The ROC curve analysis indicates that of all features in the reduction methods and normalizations, NDA is privileged over PCA and LDA in terms of differentiating between benign and malignant nodules (Figure 3, 4 and 5).

The proposed method demonstrates a more reliable performance in comparison with other studies [11-14, 22] already conducted on the subject of ultrasonic differentiation between benign and malignant thyroid nodules, with an accuracy ranging $_{from}$ 90% to 96.7%, sensitivity ranging from 88% to 94.6% and specificity ranging from 90% to 100%. In this study, we assessed all six groups of texture features and achieved higher accuracy in respect to the studies that employed one texture subset or combined some texture subsets to differentiate between benign and malignant thyroid nodules. Our

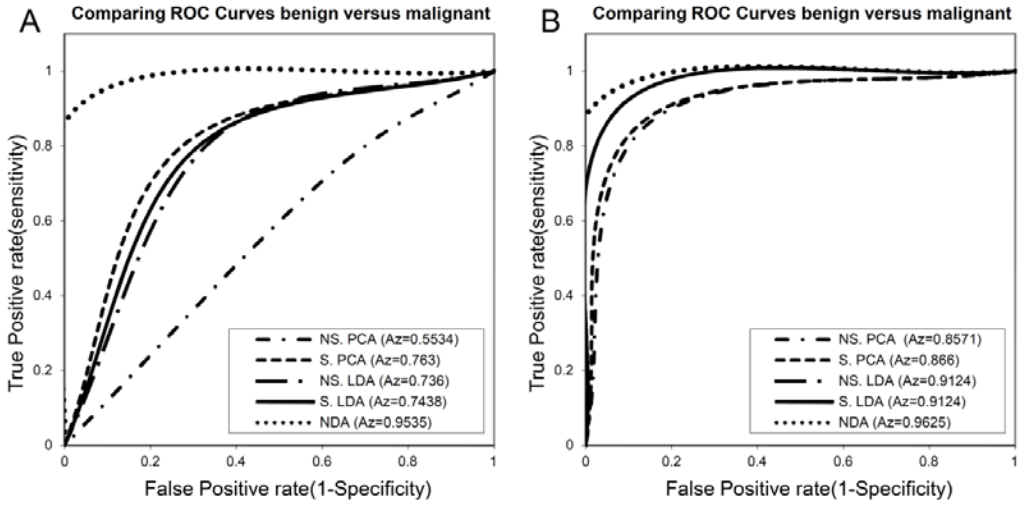

Figure 3. The diagram of the ROC curve for each texture analysis method in default. (A) Fisher features. (B) POE+ACC features.

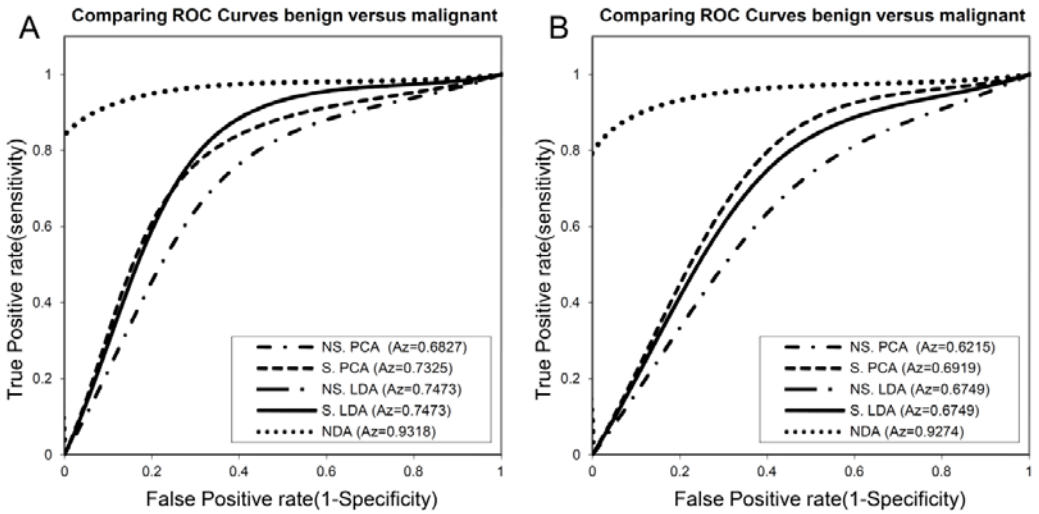

Figure 4. The diagram of the ROC curve for each texture analysis method in 3sigma normalization. (A) Fisher features. (B) POE+ACC features.

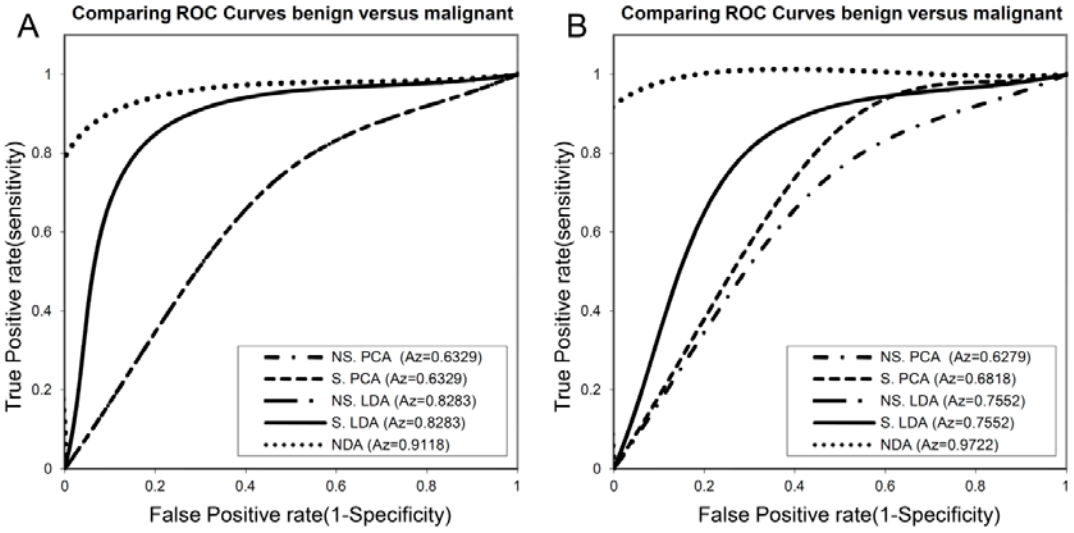

Figure 5. The diagram of the ROC curve for each texture analysis method in 1%-99% normalization. (A) Fisher features. (B) POE+ACC features.

results also indicate that texture analysis possess significantly more discriminative ability than the other methods, morphology and elastography [11, 12].

The ten texture parameters leading to the best performance in our study are as follows: Co-occurrence matrix-based features: S (0, 2) Sum entropy (S (0,2) SumEntrp) and S (1,1) Sum of squares (S (1,1) SumOfSqs) where S (i, j) shows the direction of matrix construction and inter pixel distance i along the rows and j along the columns of matrix; Energy of wavelet coefficient in 'low-high' energy components in first level wavelet decomposition (WavEnLH_s-1),'low-low' energy components in second level wavelet decomposition (WavEnLL_s-2),'low-high' energy components in third level wavelet decomposition (WavEnLH_s-3), 'low-high' energy components in fifth level wavelet decomposition (WavEnLH_s-5) and 'high-low' energy components in sixth level wavelet decomposition (WavEnHL_s-6); Absolute gradient matrix-based features: gradient Kurtosis (GrKurtosis); Auto-Regressive model: Teta1, which is the vector of AR model parameters; Histogram-based features: Kurtosis.

Our research indicates that a combination of texture features (Co-occurrence matrix, wavelet, Absolute gradient matrix, Auto-Regressive model and Histogram-based texture features) has a higher level of accuracy than the previous studies that employed one texture group [12-14, 22].

In all conditions, feature standardization affects PCA and leads to an improvement in performance. It does not have any impact on LDA except in default and Fisher features. In order to decrease the training time in ANN classifier, all input feature parameters were standardized previously in NDA.

Endocrinologist referred the cases based on clinical indication. Since this study is based on texture analysis and our gold standard is pathology, other nodule characteristic feature does not have any additional information and are not considered.

This method will not only be used as an alternative for biopsy, but also helps radiologist to select high malignancy risk of thyroid nodules for FNAB in patients with multi-nodular goiter which is the most common endocrine disease. One of the most important clinical challenges is that which nodules in patient with multi-nodular goiter should be FNAB and our methods can aid to radiologist to select the target nodule between multiple nodules in patients with multi-nodular goiter.

The main advantage of this method is that there is no operator dependency, because analysis is performed by the computer and also it does not have any additional time or costs.

In this study some limitations should be clearly noted. First, the data group was small, so further investigation with a larger data set is needed. Second, our ultrasound image classifications were performed in comparison with FNAB, although FNAB is highly sensitive for the diagnosis of neoplastic thyroid nodules, for definitive results

surgical pathology may be needed. Third, some of our data from the study were excluded due to indeterminate FNAB. Fourth, feature combination tools were not available in MaZda. For example, averaging run-length matrix features of four different orientations were hard to perform. Fifth, only nodules larger than 15 mm were used in this study, because the sizes of the ROIs for texture analysis are 12 mm × 12 mm. Sixth, in this preliminary study all the patients suspicious to thyroiditis or any other inflammatory process were excluded to avoid external perturbation of the blood flow perfusing the thyroid gland and affect texture.

Conclusion

MaZda software was originally developed in 1998 at the Institute of Electronics, Technical University of Lodz for the purpose of automatic TA of magnetic resonance imaging [15]. We also used it for ultrasound images. Generally, our results indicate that MaZda software can provide useful information contributing to the discrimination of thyroid nodules by ultrasound images, and also has the potential to help radiologists in the detection and classification of benign and malignant thyroid nodules.

Acknowledgement

This study was supported by the research bureau of the Urmia University of Medical Sciences, Urmia, Iran.

Conflicts of Interest

There is no conflict of interest in this article.

Authors' Contribution

Akbar Gharbali and Ali Abbasian Ardakani designed and analyzed the data and wrote this article. Afshin Mohammadi collected the data. All authors read and approved the final manuscript.

References

1. Sebag F, Vaillant-Lombard J, Berbis J, Griset V, Henry J, Petit P, et al. Shear wave elastography: a new ultrasound imaging mode for the differential diagnosis of benign and malignant thyroid nodules. J Clin Endocrinol Metab. 2010;95(12):5281-8.

2. Cooper DS, Doherty GM, Haugen BR, Kloos RT, Lee SL, Mandel SJ, et al. Revised American Thyroid Association management guidelines for patients with thyroid nodules and differentiated thyroid cancer: the American Thyroid Association (ATA) guidelines taskforce on thyroid nodules and differentiated thyroid cancer. Thyroid. 2009;19(11):1167-214.

3. Frates MC, Benson CB, Charboneau JW, Cibas ES, Clark OH, Coleman BG, et al. Management of Thyroid Nodules Detected at US: Society of Radiologists in Ultrasound Consensus Conference Statement 1. Radiology. 2005;237(3):794-800.

4. Chow LS, Gharib H, Goellner JR, van Heerden JA. Nondiagnostic thyroid fine-needle aspiration cytology: management dilemmas. Thyroid. 2001;11(12):1147-51.

5. Papini E, Guglielmi R, Bianchini A, Crescenzi A, Taccogna S, Nardi F, et al. Risk of malignancy in nonpalpable thyroid nodules: predictive value of ultrasound and color-Doppler features. J Clin Endocrinol Metab. 2002;87(5):1941-6.

6. Koike E, Noguchi S, Yamashita H, Murakami T, Ohshima A, Kawamoto H, et al. Ultrasonographic characteristics of thyroid nodules: prediction of malignancy. Archives of surgery. 2001;136(3):334-7.

7. Jalalian A, Mashohor SBT, Mahmud HR, Saripan MIB, Ramli ARB, Karasfi B. Computer-aided detection/diagnosis of breast cancer in mammography and ultrasound: a review. Clin Imaging. 2013;37(3):420-6.

8. Materka A, Strzelecki M. Texture analysis methods — A review. Technical University of Lodz, Institute of Electronics, COST B11 Report, Brussels. 1998.

9. Castellano G, Bonilha L, Li LM, Cendes F. Texture analysis of medical images. Clin Radiol. 2004;59(12):1061-9.

10. Materka A. Texture analysis methodologies for magnetic resonance imaging. Dialogues Clin Neurosci. 2004;6(2):243.

11. Hong Y, Liu X, Li Z, Zhang X, Chen M, Luo Z. Real-time ultrasound elastography in the differential diagnosis of benign and malignant thyroid nodules. J Ultrasound Med. 2009;28(7):861-7.

12. Tsantis S, Dimitropoulos N, Cavouras D, Nikiforidis G. Morphological and wavelet features towards sonographic thyroid nodules evaluation. Comput Med Imaging Graph. 2009;33(2):91-9.

13. Gopinath B, Shanthi N. Support Vector Machine based diagnostic system for thyroid cancer using statistical texture features. Asian Pac J Cancer Prev : APJCP. 2013;14(1):97-102.

14. Gopinath B, Shanthi N. Development of an Automated Medical Diagnosis System for Classifying Thyroid Tumor Cells using Multiple Classifier Fusion. Technol Cancer Res Treat. 2014.

15. Materka A, Strzelecki M. Texture Analysis Methods–A Review, Technical University of Lodz, Institute of Electronics, COST B11 report, Brussels (1998).

16. Schürmann J. Pattern classification: a unified view of statistical and neural approaches: John Wiley & Sons, Inc.; 1996.

17. Mucciardi AN, Gose EE. A comparison of seven techniques for choosing subsets of pattern recognition properties. Computers, IEEE Transactions on. 1971;100(9):1023-31.

18. Webb AR. Statistical pattern recognition: Wiley. com; 2003.

19. Fukunaga K. Introduction to statistical pattern recognition: Access Online via Elsevier; 1990.

20. Anderson JA, Rosenfeld E. Neurocomputing: MIT press; 1993.

21. Van Erkel AR, Pattynama PMT. Receiver operating characteristic (ROC) analysis: basic principles and applications in radiology. EJR. 1998;27(2):88-94.

22. Ding J, Cheng H, Ning C, Huang J, Zhang Y. Quantitative measurement for thyroid cancer characterization based on elastography. J Ultrasound Med. 2011;30(9):1259-66.